Nanosecond Fluorescence Spectroscopy of Human Immunoglobulin A†

Bang Maw Liu, Herbert C. Cheung,* and Jiri Mestecky

ABSTRACT: The solution properties of five samples of human immunoglobulin A (IgA) were investigated with covalent and hydrophobic fluorescence probes. The immunoglobulins included a secretory IgA and four myeloma proteins of both IgA1 and IgA2 subclasses in the monomeric and dimeric forms. The probe 8-anilinonaphthalene-1-sulfonate (ANS) was found to bind to both monomeric and dimeric IgA with comparable affinity. Pyrenesulfonyl chloride covalently linked to the proteins exhibited multiexponential decays. The decay of ANS complexed to the same proteins showed similar multiple exponential character. The rotational motions of the immunoglobulins were investigated by the nanosecond fluorescence anisotropy decay method. The decay of both probes attached to these proteins was characterized by a fast component followed by a slow component. The rapid component was in the range 14–26 ns for the covalent conjugates and 26–41 ns for the ANS complexes. These results are interpreted in terms of a segmental motion arising from a mass in the range 60 000–100 000 daltons. If the decrease in the anisotropy value at long times is taken as a measure of restricted diffusion of the mobile fragment, the half-angle of a cone within which the fragment traverses may provide a qualitative measure of the extent of flexibility. By this criterion, monomeric and dimeric IgA's of the same subclass appear to be qualitatively similar in flexibility.

Immunoglobulin A (IgA)[1] is present in human serum mainly as the 7S monomer while in external secretions it is found in a polymeric form (dimers and tetramers) associated with the secretory component (SC) (a glycoprotein, 70 000 daltons). Polymeric immunoglobulins contain a small polypeptide, the J chain (15 000 daltons), which may be required for polymer formation (Mestecky et al., 1974; Chapuis & Koshland, 1975). Secretory IgA is formed when the SC becomes linked to polymeric IgA with the J chain during its transport across epithelial cells. Since polymeric and dimeric IgA have a higher avidity and perform with a greater efficiency than monomeric IgA in many antibody functions (Heremans, 1974), it has been speculated that the poor performance of monomeric IgA might be a manifestation of the lack of flexibility in the monomer (Heremans, 1974). This difference is amenable to experimental test.

Several lines of evidence indicate that IgG is not rigid, as suggested by ultrastructural studies (Valentine & Green, 1967) and demonstrated by fluorescence anisotropy decay measurements (Yguerabide et al., 1970; Lovejoy et al., 1977). More recently, the fluorescence method was used to demonstrate that pentameric IgM in solution also possesses segmental flexibility (Holowka & Cathou, 1976). These fluorescence studies used specific fluorescent haptens as molecular probes. In attempts to demonstrate segmental flexibility in human myeloma and secretory IgA proteins, one encounters the problem that no haptenic activity has been observed in these immunoglobulins. The lack of known haptenic activity prevents the use of specific fluorescent probes as has been done with IgG and IgM and necessitates the use of either covalent or hydrophobic probes. Nonspecific covalent probes were used in early studies of IgG (Wahl & Weber, 1967; Weltman & Edelman, 1967; Brochon & Wahl, 1972) and IgM (Knopp & Weber, 1969) before specific fluorescent haptens were used. Such nonspecific covalent probes continue to be useful for IgG (Tumerman et al., 1972; Dudich et al., 1978) although IgG against specific haptens with different fluorescent moieties can now be easily obtained. Becuase of the lack of specific haptenic activity in human IgA, we carried out a preliminary nanosecond fluorescence study of a 7S myeloma IgA which was labeled with dansyl chloride (Liu et al., 1977). The results were compatible with the notion that the protein is segmentally flexible. It is important to ascertain whether the observed flexibility is a general property of this class of human immunoglobulins. In the present study, we have extended our fluorescence study to include a secretory IgA and four myeloma IgA proteins with different structural and molecular forms. These proteins were investigated with two different fluorescent probes. The myeloma proteins belonged to both IgA1 and IgA2 subclasses and were monomeric and dimeric. The results provide evidence suggesting that molecular flexibility may well be a general property of the IgA class of immunoglobulins.

Materials and Methods

IgA1 and IgA2 proteins were isolated from the plasma of patients with multiple myeloma proteins. The isolation and characterization of these proteins have been reported (Mestecky et al., 1977). SIgA was isolated from pooled colostrum and prepared as described previously (Mestecky et al., 1972). Pertinent information on these proteins is given in Table I. Fab and Fc fragments of IgA1 were obtained by cleavage with IgA1 protease prepared from *Streptococcus sanguis* (ATCC 10556). The proteolytic fragments were separated, and the Fab and Fc fragments were immunologically identified as previously described (Kilian et al., 1979). Pyrenesulfonyl chloride was purchased from Sigma Chemical Co. (St. Louis, MO), and 8-anilinoanaphthalene-1-sulfonate was obtained from Eastman Organic Chemicals (Rochester, NY) in the form of the magnesium salt. These probes were used without further purification.

In a typical experiment, we started with a solution of IgA which had been stored in the frozen state or lyophilized IgA that was first suspended in 0.1 M $NaHCO_3$ and then the

† From the Biophysics Section, Department of Biomathematics (B.M.L. and H.C.C.), and the Department of Microbiology (J.M.), University of Alabama in Birmingham, University Station, Birmingham, Alabama 35294. *Received January 15, 1980.* This work was supported in part by Grants AM-14589 and AI-10854 from the National Institutes of Health.

[1] Abbreviations used: IgA, immunoglobulin A; IgM, immunoglobulin M; IgG, immunoglobulin G; SIgA, secretory immunoglobulin A; SC, secretory component; Tris, tris(hydroxymethyl)aminomethane; PYS, pyrenesulfonyl chloride; ANS, 8-anilinonaphthalene-1-sulfonate.

0006-2960/81/0420-1997$01.25/0

Table I: Characteristics of Human IgA Proteins[a]

sample	subclass	L chain type	J chain presence	$s_{20,w}$	molecular form
KNI	IgA1	κ	−	7.2	monomer
JL[b]	IgA1	κ	+	9.1	dimer
CAR	IgA1	κ	+	9.5	dimer
FEL	IgA2	κ	+	9.5	dimer
SIgA[c]		κ, λ	+	11.0	dimer and tetramer

[a] Mestecky et al. (1977). The symbols used here for the samples are different from those used in the original paper. [b] From patients with hyperviscosity syndrome. [c] Heterogeneous—the preparation contains approximately 20% of tetramer (15S) SIgA.

undissolved material was removed. Prior to being labeled, the protein was dialyzed against 0.05 M Tris and 0.15 M NaCl at pH 8.0. The probe PYS was first dissolved in acetone, and the resulting solution was added dropwise to the protein solution under stirring. The volume of the acetone solution added was less than 5% of the final volume. The resulting mixture, in which the molar ratio of probe to protein was always less than 2, was incubated at 4 °C overnight. Unreacted probe was removed by exhaustive dialysis against the Tris–NaCl buffer. The degree of labeling was determined from the absorbance of the protein at 280 nm by using $A^{1\%}_{280nm} = 14.0$ cm^{-1} (Brandtzaeg, 1975) and the absorbance of the probe at its absorption peak. The extinction coefficients used were 54000 M^{-1} cm^{-1} at 335 nm for PYS (Berlman, 1971) and 5800 M^{-1} cm^{-1} at 350 nm for ANS (Cheung & Morales, 1969). The molecular weights used for the proteins were 160000 for monomeric IgA without the J chain, 350000 for dimeric IgA with the J chain, and 420000 for SIgA (Björk & Lindh, 1974). Except for sample KNI which had been lyophilized, the other samples were stored in the frozen state. It is our experience that there were no gross changes in these or other frozen immunoglobulin samples upon long-term storage as evidenced by gel electrophoresis and sedimentation patterns. By the same criteria, we found no gross changes in the solutions of lyophilized samples, provided that they were first centrifuged to remove undissolved materials.

Steady-State Fluorometry. Fluorescence emission spectra were recorded in a ratio spectrofluorometer previously described (Habercom & Cheung, 1978). Corrected emission spectra were obtained at 25 °C by the method of Melhuish (1962). Pyrenylated IgA was excited at 335 nm, and the ANS–IgA complexes were excited at 350 nm.

The binding of ANS to the proteins was determined in fluorescence titration experiments at 25 °C by using a Corning 3-72 filter (cutoff wavelength 410 nm) to isolate the emission at a right angle. Initially, the titrations were carried out with a fixed concentration of ANS, and the number of binding sites was estimated from this set of data. The titrations were then repeated by fixing the protein concentration and varying the ANS concentration. The number of binding sites (n) and the intrinsic association constant (k) were first obtained from the Scatchard plot (Scatchard, 1949) $r/A = kn - kr$, where r is the molar ratio of bound ANS to protein and A is the free ANS concentration. These initial parameters (n and k) were then used to reevaluate the binding data by a procedure of nonlinear least squares according to the following equation: $r = nkA/(1 + kA)$ (Klotz, 1974).

Nanosecond Fluorometry. Fluorescence lifetime and fluorescence anisotropy decay were determined at 25 °C (unless stated otherwise) in a photon-counting pulsed fluorometer previously described (Harvey & Cheung, 1977), with an air-cooled spark gap light source pulsed at about 50000 Hz. The excitation wavelength was 336 nm for PYS and 350 nm for ANS. A cutoff Corning 3-72 filter was used to isolate the probe fluorescence. Polaroid HNP'B sheets were employed to provide polarized excitation and to isolate the two mutually perpendicular components of the polarized emission. In lifetime experiments, data collection was stopped when the total counts reached about 10^6 with a sample rate of 2500 Hz. For anisotropy decay measurements, the two polarized components of the polarized emission were recorded semiconcurrently with two photomultiplier tubes located on both sides of the sample cell. It was found that a total photon count in the range (8–12) $\times 10^6$ was needed to provide a smooth anisotropy decay curve.

Lifetime data were deconvoluted with a computer program based on a nonlinear least-squares method (Marquardt, 1963). The program included corrections (Grinvald, 1976) for nonrandom errors introduced by sample light scattering and zero time shift of the detector systems (Wahl et al., 1974). Three criteria were used to judge the goodness of fit between chosen decay functions and observed data (Grinvald, 1976; Gafni & Brand, 1976): (1) the reduced χ square ratio, χ_R^2, (2) the autocorrelation function of the residuals, and (3) the weighted residual plot.

The fluorescence anisotropy decay was calculated from the equation

$$r(t) = \frac{I_{\parallel}(t) - I_{\perp}(t)}{I_{\parallel}(t) + 2I_{\perp}(t)} \quad (1)$$

where $I_{\parallel}(t)$ and $I_{\perp}(t)$ are the components of emission observed with the analyzer parallel and perpendicular to the direction of polarization of the excitation light, respectively. The procedure used to calculate $r(t)$ from $I_{\parallel}(t)$ and $I_{\perp}(t)$ was similar to that described previously (Harvey & Cheung, 1977).

Rotational Brownian motion of a fluorophore is known to have an effect on its apparent lifetime (Shinitzky, 1972). Two methods can be applied to eliminate this effect: (1) exciting with natural light and measuring the emission at 55° relative to the incident beam or (2) vertically polarizing the excitation and observing the emission at a right angle with a polarizer oriented at 55° relative to the excitation polarization. One experiment was performed by using the second method. The results indicate that the effect of Brownian rotation was negligible for the system studied; no polarizer was used in the other experiments.

The decay curve of fluorescence anisotropy contains information bearing on the structure of the rotating particle. The functional form of this decay curve is a sum of five exponential terms for a rigid particle of arbitrary shape:

$$r(t) = \sum_{i=1}^{5} B_i \exp(-t/\phi_i) \quad (2)$$

The rotational correlation times, ϕ_i, depend on the rotational diffusion coefficients, which, in turn, depend on the size and the shape of the molecule, temperature, and solvent viscosity. The coefficients, B_i, depend on the orientations of the absorption and emission dipoles in the molecule. If the molecule can be approximated by a rigid ellipsoid, eq 2 reduces to three exponential terms. The correct relationships between the parameters of eq 2 and the molecular parameters are given by Belford et al. (1972), Ehrenberg & Rigler (1972), and Chuang & Eisenthal (1972).

While the anisotropy decay curve for a rigid molecule is theoretically multiexponential (unless it has spherical symmetry), in practice only one exponential term frequently suffices to describe the data because of the inability of the experimental technique to detect correlation times longer than

Table II: Fluorescence Lifetimes of PYS–IgA Conjugates Derived from Triexponential Fits[a]

sample	concn (mg/mL)	PYS/IgA[b]	α_1	τ_1 (ns)	α_2	τ_2 (ns)	α_3	τ_3 (ns)	χ_R^2
KNI	1.0	0.8	0.73 ± 0.04	3.7 ± 0.3	0.17 ± 0.02	14.1 ± 3.0	0.10 ± 0.02	41.4 ± 3.7	2.2
JL	1.4	0.4	0.86 ± 0.02	2.7 ± 0.3	0.10 ± 0.03	18.4 ± 0.2	0.04 ± 0.01	37.9 ± 3.2	2.7
JL[c]	1.4	0.4	0.88 ± 0.01	3.2 ± 0.2	0.09 ± 0.01	17.1 ± 4.0	0.03 ± 0.02	46.0 ± 13	3.1
CAR	1.0	0.5	0.80 ± 0.01	3.5 ± 0.2	0.14 ± 0.02	17.8 ± 4.2	0.06 ± 0.03	48.9 ± 16	1.9
FEL	1.0	0.7	0.89 ± 0.04	3.3 ± 0.01	0.07 ± 0.01	12.5 ± 3.2	0.04 ± 0.01	39.0 ± 3.6	2.5
SIgA	1.1	1.1	0.90 ± 0.01	3.4 ± 0.1	0.07 ± 0.01	17.2 ± 0.1	0.03 ± 0.01	49.5 ± 0.5	3.0

[a] Parameters are averages of two experiments. See text for other conditions. [b] Molar ratio. [c] Measured with vertically polarized excitation and emission polarized at 55° with respect to the direction of polarized excitation.

1000 ns. If a molecule can be assumed to be flexibile, then a second correlation time may be indicative of internal flexibility.

For segmentally flexible macromolecules, there exists a simple model where the fluorophore is assumed to be randomly oriented on a segment, the rotational motion of which is independent of the molecular motion of the entire molecule. This model is given by eq 3 where the correlation time ϕ_f (fast) is

$$r(t) = r_f \exp(-t/\phi_f) + r_s \exp(-t/\phi_s) \quad (3)$$

assigned to the segmental motion and ϕ_s (slow) to the overall motion of the whole molecule (Yguerabide et al., 1970). The coefficient r_s is a measure of the angle traversed by the segment.

An alternate model for segmental flexibility is one in which a small ellipsoidal fragment is assumed to rotate on top of a large spherical mass, and the motion of the fragment is superimposed on that of the heavy mass. This model is given by eq 4 where the coefficients B_i refer to those of the small

$$r(t) = [\sum_{i=1}^{3} B_i \exp(-t/\phi_i)] \exp(-t/\phi_{sp}) \quad (4)$$

ellipsoid with correlation times ϕ_i, and ϕ_{sp} is the correlation time of the heavy mass approximated by a sphere (Gottlieb & Wahl, 1963; Rigler & Ehrenberg, 1976).

Results

Steady-State Spectral Distribution. The emission spectra of PYS covalently attached to the five IgA proteins showed the usual fine structure of pyrene with two sharp peaks at about 380 and 405 nm and a shoulder at 420 nm. No evidence of excimer emission was observed with the pyrenylated proteins. The sepctra of ANS complexed with the proteins showed a typical single broad peak in the region 470–480 nm, indicating the similarity and relatively nonpolar nature of the binding sites.

Binding of ANS to IgA. The binding of ANS to two myeloma proteins (KNI and FEL) was studied over a wide range of ligand concentrations. A typical set of binding data is shown in Figure 1, which indicates a single set of binding sites with n approximately equal to 1. From the results of three separate experiments, the following values of the intrinsic binding constant (k) and the number of binding sites per protein molecule (n) were obtained: $k = 1.1 \times 10^6$ M^{-1} and $n = 1.1$ for ANS–KNI; $k = 1.2 \times 10^6$ M^{-1} and $n = 1.3$ for ANS–FEL. These results show similar binding properties of both monomeric and dimeric proteins.

Analysis of Fluorescence Lifetime Results. The lifetime date of PYS covalently conjugated to the five proteins were clearly not monoexponential. The best biexponential fit of PYS–KNI is shown in Figure 2a. This fit is characterized by a large χ_R^2 (12.7) and unacceptable autocorrelation function and weighted residual plots. The fitting is considerably improved with a triexponential function, yielding three lifetimes, as shown in Figure 2b. The results obtained from

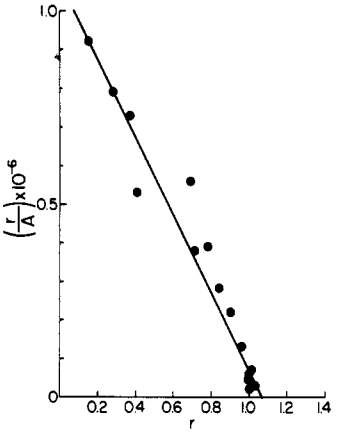

FIGURE 1: Scatchard plot of ANS binding to IgA1 (KNI), with protein concentration held at 1×10^{-5} M. The symbol r represents moles of ANS bound per mole of protein, and A is free ANS concentration. The correlation coefficient from linear regression is 0.95. See text for other conditions.

triexponential fits of the PYS conjugates are given in Table II. The complexity of the decay pattern might arise from Brownian rotational motion of the protein molecule if such motion occurred within the lifetime scale. It seems unlikely that rotational mobility was responsible for the observed decay since the same results were obtained with one sample whether the measurement was made with unpolarized light or with polarized excitation and emission polarized at the "magic angle" of 55°.

In an attempt to obtain some indication of the location of the PYS probe, PYS-labeled IgA1 was cleaved by IgA1 protease, and the resulting Fab and Fc fragments were isolated. From both the absorbance at 355 nm and the integrated emission intensity measured with 335-nm excitation, about 95% of the PYS was found to be associated with the Fab fractions and the remaining 5% with the Fc fractions. This result indicates that the predominant location of the probe in the intact IgA1 was the Fab moiety.

The lifetime of ANS bound to the IgA proteins was measured at a probe/proteins molar ratio of 0.86 and, in addition, at a ratio of 0.43 for one sample (FEL). All decay curves are reasonably fitted to biexponential functions, yielding two lifetimes in the range 4–18 ns. These results are summarized in Table III. Although a small fraction of ANS in all these samples was unbound, its contribution to the observed decay was negligible since free ANS in water solution has a quantum yield 100-fold smaller than that in a nonpolar environment.

Fluorescence Anisotropy Decay of IgA. The anisotropy decay curves of PYS conjugated to IgA and of ANS complexed to these proteins are all characterized by an initial fast decay component followed by a slowly decreasing component. Typical decay curves for PYS–KNI and ANS–KNI are depicted in Figures 3 and 4, respectively. Decay parameters derived from the decay curves of the PYS conjugates are listed

Table III: Fluorescence Lifetimes of ANS–IgA Complexes Derived from Biexponential Fits[a]

sample	concn (mg/mL)	ANS/IgA[b]	α_1	τ_1 (ns)	α_2	τ_2 (ns)	χ_R^2
KNI	1.0	0.86	0.58 ± 0.02	5.7 ± 0.3	0.42 ± 0.02	18.7 ± 0.3	2.3
JL	1.4	0.86	0.69 ± 0.02	4.8 ± 0.2	0.31 ± 0.01	17.1 ± 0.3	2.3
CAR	1.0	0.86	0.71 ± 0.03	4.9 ± 0.3	0.29 ± 0.02	16.6 ± 0.4	2.8
FEL	1.0	0.86	0.71 ± 0.03	4.7 ± 0.2	0.29 ± 0.01	17.5 ± 0.3	3.1
FEL	1.0	0.43	0.69 ± 0.02	5.0 ± 0.2	0.31 ± 0.01	17.3 ± 0.2	1.8
SIgA	1.0	1.0	0.70 ± 0.03	4.0 ± 0.3	0.30 ± 0.02	16.5 ± 0.5	2.0

[a] Parameters are averages of two experiments. See text for other conditions. [b] Molar ratio.

Table IV: Fluorescence Anisotropy Decay Parameters of PYS–IgA Conjugates[a]

sample	concn (mg/mL)	PYS/IgA[b]	r_1	ϕ_1 (ns)	r_2	ϕ_2 (ns)	χ_R^2
KNI	1.0	0.8	0.120 ± 0.005	14.6 ± 1.2	0.050 ± 0.005	>1000	1.7
JL	1.4	0.4	0.157 ± 0.009	16.4 ± 1.7	0.035 ± 0.010	>1000	1.6
CAR	1.0	0.5	0.155 ± 0.007	15.2 ± 1.6	0.045 ± 0.009	>1000	1.7
FEL	1.0	0.7	0.202 ± 0.011	17.8 ± 2.1	0.045 ± 0.009	>1000	1.6
SIgA	1.1	1.0	0.234 ± 0.010	26.3 ± 2.4	0.056 ± 0.011	>1000	2.2

[a] Parameters are averages of two experiments. See text for other conditions. [b] Molar ratio.

Table V: Fluorescence Anisotropy Decay Parameters of ANS–IgA Complexes[a]

sample	concn (mg/mL)	ANS/IgA[b]	r_1	ϕ_1 (ns)	r_2	ϕ_2 (ns)	χ_R^2
KNI	1.0	0.86	0.134 ± 0.051	41.3 ± 3.3	0.092 ± 0.051	>1000	1.5
JL	1.4	0.86	0.078 ± 0.007	38.3 ± 6.9	0.119 ± 0.009	>1000	1.6
CAR	1.0	0.86	0.112 ± 0.009	34.3 ± 9.0	0.106 ± 0.010	>1000	1.7
FEL	1.0	0.86	0.049 ± 0.009	33.2 ± 7.6	0.138 ± 0.009	>1000	2.1
SIgA	1.0	0.86	0.025 ± 0.008	26.3 ± 17.0	0.173 ± 0.008	>1000	3.0

[a] Parameters are averages of two experiments. See text for other conditions. [b] Molar ratio.

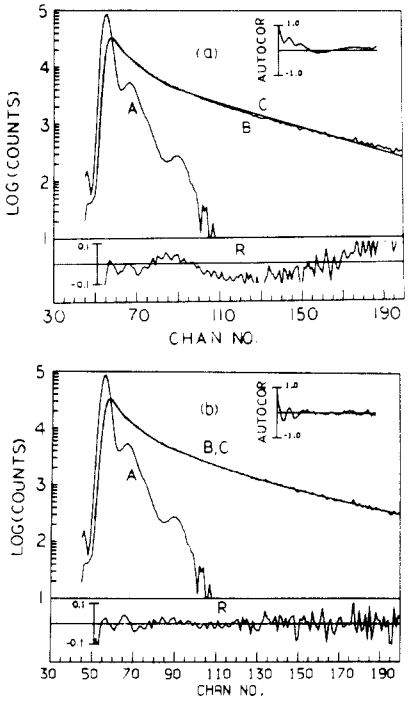

FIGURE 2: Fluorescence decay of PYS–KNI conjugate. Protein concentration was 1 mg/mL in 0.05 M Tris and 0.15 M NaCl, pH 8, 25 °C. The degree of labeling was 0.8. Curves A, B, and C are the lamp profile, experimental curve, and best fitted curve, respectively. Also shown are the autocorrelation function and the weighted residual (R) plots. (a) Biexponential fit, $\chi_R^2 = 12.7$. (b) Triexponential fit, $f(t) = \alpha_1 \exp(-t/\tau_1) + \alpha_2 \exp(-t/\tau_2) + \alpha_3 \exp(-t/\tau_3)$. Best fitted parameters are the following $\alpha_1 = 0.81 \pm 0.04$, $\tau_1 = 3.6 \pm 0.2$ ns; $\alpha_2 = 0.14 \pm 0.02$, $\tau_2 = 17.9 \pm 4.8$ ns; $\alpha_3 = 0.05 \pm 0.03$, $\tau_3 = 47.9 \pm 12.4$ ns; $\chi_R^2 = 3.0$. Time scale: 0.796 ns/channel.

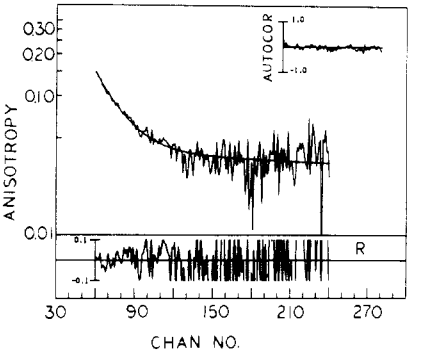

FIGURE 3: Fluorescence anisotropy decay of PYS–KNI conjugate at 1 mg/mL. See Figure 1 for experimental conditions. The best parameters derived from a biexponential function are as follows: $r_1 = 0.109 \pm 0.006$, $\phi_1 = 15.1 \pm 1.4$ ns; $r_2 = 0.039 \pm 0.006$, $\phi_2 > 1000$ ns; $\chi_R^2 = 1.3$. Time scale: 0.857 ns/channel.

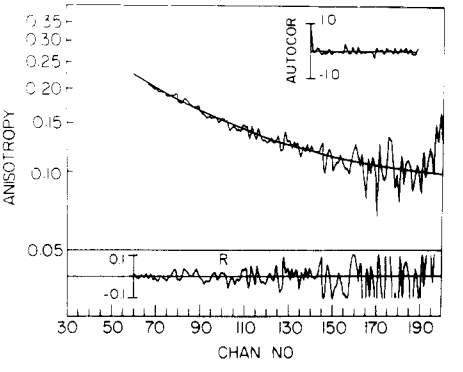

FIGURE 4: Fluorescence anisotropy decay of ANS–KNI complex at 1 mg/mL. The ANS/protein ratio was 0.86. See Figure 1 for experimental conditions. The best parameters derived from the biexponential fit are the following: $r_1 = 0.130 \pm 0.007$, $\phi_1 = 39.2 \pm 3.7$ ns; $r_2 = 0.097 \pm 0.007$, $\phi_2 > 1000$ ns; $\chi_R^2 = 1.8$. Time scale: 0.796 ns/channel.

in Table IV, and those from the ANS complexes are given in Table V. In spite of the relatively large scatter in the data

points in the tail region of the decay curves, it is clear that the decays are not monoexponential. Since satisfactory fits were obtained with biexponential functions in all cases, we did not feel justified to attempt triexponential fits. Except for SIgA, the fast components (ϕ_1) of the ANS complexes are 2–3 times slower than those of the PYS conjugates. The slow component (ϕ_2) is too slow to be resolved by the present method.

The generally smaller values of ϕ_1 observed with PYS as compared with those observed with ANS might be due to some probe mobility in the PYS conjugates. If the attached PYS moiety was indeed somewhat mobile, the smaller value of ϕ_1 might reflect an average of probe mobility and some type of protein mobility. Since ANS is a probe which interacts in a hydrophobic environment through multiple points of attachment, the ϕ_1 values observed with the ANS complexes should reflect entirely the molecular properties of the protein itself. This expectation is borne out by the considerably larger ϕ_1 of the ANS complexes. Although we were unable to place an estimate in ϕ_2 of the PYS conjugates and ANS complexes, the value of ϕ_1 suffices to provide information on segmental flexibility as will be made clear.

Discussion

Binding of 8-Anilinonaphthalene-1-sulfonate to IgA. ANS binds to both human monomeric and dimeric IgA in a relatively nonpolar region. There appears to be only one binding site in both proteins with comparable binding affinity. These results are different from those reported by Rosenstein & Jackson (1973) on mouse myeloma IgA (MOPC 460), which interacts with ANS only in the dimeric form. No information was obtained in their study regarding the rotational mobility of the protein. That one binding site is found for both monomer and dimer suggests the possibility that the ANS site on a second monomer becomes inaccessible upon dimerization and that the site is unlikely to be located in the Fab arms. It also appears unlikely that the J chain is involved in the ANS binding to the dimer since the binding affinity is independent of the molecular form.

Multiple Lifetimes. Both probes used to investigate the solution properties of the five IgA proteins exhibit multiple lifetimes when attached to the proteins. The shortest component ranges from 3–4 ns in the case of PYS to 4–6 ns for ANS. This short time constant is of the same order of magnitude as the width of the exciting lamp pulses and could reflect scattering of the exciting light that was sensed by the detector. This possibility is considered unlikely for the following reasons. (1) All protein samples were clarified and had no visible turbidity; light scattering from these solutions should not be appreciable. (2) The cutoff filters that were used to isolate the probe emission were of such spectral qualities that the exciting light at 336 or 350 nm was either completely blocked or transmitted only to the extent of a very small fraction of 1%. (3) A scattering factor was included in the computer program for data deconvolution. Any scattered light that reached the detector would have been corrected for by the deconvolution procedure. These considerations indicate that any residual scattered light that was still present in the reduced data could not be more than a small fraction of the total signal. In every case, the observed short lifetime represents over 50% of the total signal ($\alpha_1 > 0.5$), and there is no reasonable way to reconcile it with scattered light. The cutoff filters were made of colored substances which could possess a small amount of visible fluorescence. This stray signal can be eliminated by adding a nonfluorescent Corning 3-144 filter next to the emission filter. The addition of this filter had no significant effect on the reduced data.

A second possible origin of multiple PYS lifetimes could be heterogeneous labeling of the proteins. This possibility cannot be completely ruled out although the degree of labeling was kept close to one, and, as has been indicated under Results, about 95% of the PYS probe attached to IgA1 was localized in the Fab moiety. This finding, however, does not rule out heterogeneous labeling.

In the case of the ANS complexes, the simple Scatchard analysis does not support two sets of ANS binding sites. The long lifetime (τ_2) observed with the five ANS complexes is typical of this probe bound to a number of other proteins. If the short lifetime τ_1 reflects the presence of unbound ANS, reduction of the probe/protein ratio from 0.86 to 0.43 will shift the ANS–IgA equilibrium in favor of the bound species and should decrease the coefficient (α_1) associated with the short lifetime. The observed value of α_1, however, remains unchanged at 0.7. It should be clear from the intrinsic binding constant which was determined in the present work that a value of $\alpha_1 = 0.7$ can in no way be due to unbound ANS. This and other observations discussed above are strong indications that the multiple lifetimes observed in the present study reflect the solution properties of the probe–immunoglobulin complexes. The present data are insufficient to provide a more rigorous interpretation of the origin of multiple ANS lifetimes, however.

There remains the possibility that multiple exponential decay is due to excited-state interactions in which the emission kinetics are dependent upon the emission wavelength (Gafni & Brand, 1976). Of the two probes used, only PYS might possess this property since it shows a complex-structural emission spectrum. This possibility can be ruled out since there was only one probe or less attached to each protein, and the concentrations of the conjugates were sufficiently low to even allow excimer formation.

Existence of Segmental Flexibility. If one assumes monomeric IgA to be a spherical rotor (M_r = 160 000) with a specific volume ($\bar{v}$) of 0.75 cm^3 g^{-1} and a degree of hydration (h) of 0.20, its theoretical rotational correlation time is calculated to be 62 ns at 25 °C. This value is considerably smaller than the observed ϕ_2 (>1000 ns) and longer than the observed ϕ_1 (14–40 ns) for monomeric PYS–KNI and ANS–KNI. Similar calculations show that all five IgA proteins cannot be approximated by a rigid spherical model.

In Figure 5, the observed anisotropy decay curves of PYS–KNI and ANS–KNI are compared with the theoretical curves for rigid ellipsoidal molecules. These curves were calculated by using eq 2 with i = 1, 2, and 3 and the following assumptions: (1) $\bar{v} = 0.75$ and $h = 0.20$, (2) the absorption and emission dipoles have the same colatitude angle, 30°, and (3) the angle between the two dipoles is 30° as deduced from the experimental values of $r(0)$. The pronounced curvature displayed in both experimental curves is incompatible with the theoretical model of rigid ellipsoidal molecules with an axial ratio in the range 1–5. The discrepancy cannot be removed by varying the colatitude angle. It has been shown that the smallest correlation time of a rigid ellipsoid cannot be smaller than $0.95\phi_0$, where ϕ_0 is the theoretical correlation time of an equivalent sphere (Tao, 1969). The values of ϕ_0 are 58, 131, and 139 ns for monomeric IgA, dimeric IgA, and SIgA, respectively. The observed value of ϕ_1 in all three cases is less than $0.95\phi_0$. When these considerations are taken together, it becomes clear that the present anisotropy decay results are not compatible with a model of a rigid ellipsoidal rotor.

Having ruled out a rigid structure, it may be assumed that the short correlation time arises from the motion of a small

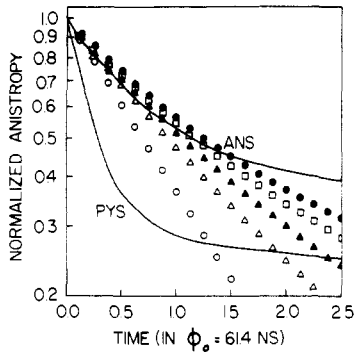

FIGURE 5: Comparison of measured anisotropy decay curves of PYS–KNI and ANS–KNI with theoretical decay curves based on a rigid ellipsoidal model. Normalized anisotropy is plotted as a function of ϕ_0, which is the theoretical rotational correlation time for a rigid equivalent sphere. Experimental curves (solid lines) are taken from Tables IV and V, and the theoretical curves are calculated for various values of the following axial ratios: 1.0 (○), 2.0 (△), 3.0 (▲), 4.0 (□), and 5.0 (●).

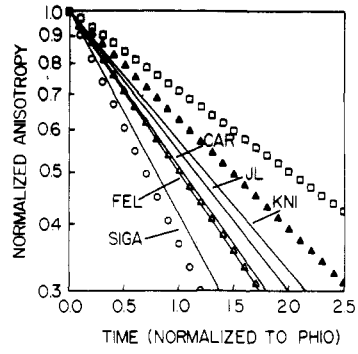

FIGURE 6: Calculated anisotropy decay characterizing segmental motion compared with the fast mode of motion of the ANS complexes. The experimental data (solid curves) are taken from Table V. The theoretical curves are calculated from eq 3, by assuming a rigid ellipsoidal segment rotating independently of the motion of the rest of the molecule with the following axial ratios: 1.0 (○), 2.0 (△), 3.0 (▲), and 4.0 (□). The abscissa is the same as that in Figure 4.

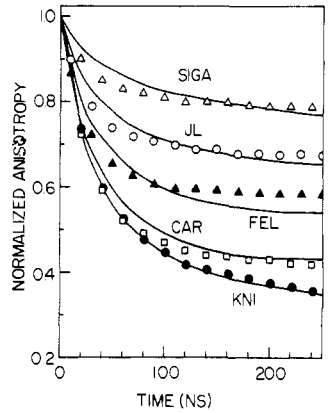

FIGURE 7: Calculated anisotropy decay characterizing segmental motion according to eq 4 with a 60 000-dalton fragment undergoing torsional motion on top of a heavy spherical mass. The calculated peak-normalized anisotropy (symbols) for each protein is compared with the corresponding observed ANS decay (solid curve). For these calculations, the following values are assumed: $\bar{v}$ = 0.75 mL g^{-1}, h = 0.30. In addition, the angle δ used for the five proteins KNI, JL, FEL, CAR, and SIgA is 36, 41, 39, 35, and 43°, respectively. The corresponding values for the colatitude angle ψ_3, θ_3 are 75, 85, 85, 80, and 85°. The angle δ is measured between the absorption and emission dipoles. The colatitude angle is measured from the transition dipole to the major axis of the ellipsoidal fragment with an axial ratio of 2.

spherical or ellipsoidal fragment which either is externally linked to the protein (such as a covalent probe) or is a part of the protein. If the motion of the small fragment is independent of that of the entire molecule, the simple model represented by eq 3 can be used to model the observed decay. If the same specific volume (0.75) and hydration (0.20) are assumed, the mass responsible for the short correlation time (14 ns) observed with PYS–KNI is calculated to be 35 000–60 000 daltons. The short correlation time (26 ns) obtained from SIgA can be similarly interpreted. The larger ϕ_1 of SIgA may reflect either its larger molecular weight in comparison with the other immunoglobulins or a distinctly different labeling site (i.e., Fc or SC). The present results do not allow a distinction between these possibilities.

The calculated mass of the mobile fragment suggests that the short correlation time cannot be due to a mobile probe. Although it is unrealistic to expect the rotational motion of the covalently attached PYS to be totally free, it seems unlikely that even a restricted rotation could give rise to a correlation time as long as 14 ns. A survey of the literature shows that the correlation time of a probe restricted on a protein surface is on the order of 1–4 ns. The possibility of probe motion can be ruled out with some confidence when the correlation times of ANS complexes are considered. For these hydrophobic complexes, the short correlation times are in the range 26–42 ns. Since ANS is relatively planar and its interaction within a hydrophobic crevice is likely to involve multiple points of attachment, the observed short correlation time cannot be due to probe motion. The long correlation time reflects the overall macromolecular motion, and this correlation time is compatible with our knowledge that IgA is highly asymmetric. This mobile fragment as deduced from the short correlation time is 66 000–105 000 for ANS–IgA. Again, the fragments are too large to be attributed to the probe.

The range of the observed values of ϕ_1 is comparable to the short correlation time (33 ns) that was observed with rabbit antidansyl IgG (Yguerabide et al., 1970) and antipyrene IgG (Lovejoy et al., 1977). In these studies, the fluorescence probes were used as specific haptens, while in the present work the probe locations were not known. A semiquantitative test of eq 3 is shown in Figure 6, where the observed fast anisotropy decay components of the ANS complexes are compared with theoretical curves expected of a rigid ellipsoidal fragment of $\bar{M}_r$ 60 000. The results show that the observed fast decay can be reasonably approximated by the motion of a fragment the size of which is similar to Fab and with an axial ratio of 1.5–2.5.

Equation 4 describes a model which differs from eq 3 in that the motion of the mobile fragment is not independent of the rest of the macromolecule. In this model, an ellipsoidal fragment is allowed to undergo rapid torsional motion only (with correlation times ϕ_i) relative to the rest of the molecule which is approximated by a rigid sphere with a long correlation time ϕ_{sp} ($D_\perp = 0$, $\phi_{sp} \simeq \infty$). The computed curves according to eq 4 are compared with the observed curves in Figure 7. A good agreement between the model and the data for all five ANS–IgA complexes is clearly demonstrated.

The agreement between the observed data and the two flexibility models leads us to conclude that IgA is a flexible rotor and that the segmental motion can arise from a fragment of considerable mass. In the case of IgA1, the mobile fragment appears to be the Fab moiety as the pyrene probe was found localized predominantly on the Fab fragment. It is less certain as to which portion of IgA2 is mobile. The location of the mobile fragment in both IgA1 and IgA2 that is sensed by ANS cannot be ascertained because of the uncertainty of probe location. This difficulty, however, does not invalidate the

conclusion that IgA is not rigid. The conclusion does not depend upon knowledge of probe location although it certainly would allow a more rigorous interpretation of the ANS anisotropy decay results. The present finding adds to our knowledge that IgG and IgM are flexible. The conclusion of the present work differs from that of Weltman & Davis (1970), who showed that the anisotropy decay curve of a human myeloma IgA protein (10.4 S) covalently linked to dansyl chloride appeared to monoexponential. Their data were not subjected to biexponential fits, and no statistical criterion was used to indicate that the observed data were indeed best fitted to a single exponential function. A close examination of their anisotropy decay curve reveals an initial curvature which was apparently dismissed by the authors as not of any significance. In this connection, we extended our previous work (Liu et al., 1977) of the myeloma protein KNI labeled with dansyl chloride to include the other four proteins which were investigated with PYS and ANS. The results on these dansyl conjugates (not reported here) showed two lifetimes and biexponential anisotropy decay. The latter results are in qualitative agreement with those reported here.

Upon examination of Table IV, one finds striking differences in the coefficients associated with the two correlation times among the five conjugates. If the small fragment associated with the short rotational correlation time were isolated and removed from the rest of the protein molecule, its anisotropy decay pattern would be expected to be similar to the fast component that was observed with the intact molecule, with the exception that the anisotropy of the isolated fragment should decay to zero within the time scale of the experiment. The fact that the decay data do not decay to zero suggests a hindered rotation. As has been pointed out (Dale & Eisinger, 1975), the decrease of $r(t)$ from its value at zero time to a plateau value at a long time can be related to the angular range over which the fluorophore is constrained to move. From the observed reduction in anisotropy, the half-angle of the cone traversed by the emission dipole fixed on a fragment can be calculated, and this angle might serve to indicate the extent of fragmental flexibility. Although quantitative comparison of this angle for the five samples is not carried out, it is noted that among the PYS–IgA1 samples there is no large difference in the values of r_1 and r_2, thus suggesting that the extent of restricted fragment motion is qualitatively similar.

It is known that monomeric IgA is a poor agglutinin, while the polymeric and secretory forms of IgA are more efficient in this function. Our fluorescence results indicate that there is no lack of flexibility in monomeric IgA. The poor performance of monomeric IgA in a number of biological functions does not appear to correlate with the type of flexibility which is reported in the present study. Other factors such as carbohydrate content and possible interaction between antigen binding sites might be important factors to be considered in explaining the difference in performance.

Acknowledgments

We are indebted to Dr. F. Garland for discussion on nonlinear regression techniques and to Dr. S. Harvey for discussion on several aspects of this work relating to the general problem of macromolecular flexibility. We also thank R. Kulhavy for the preparation of IgA samples. Acknowledgment is extended to the staff of the Josiah Macy, Jr., Research Computer Center at the University of Alabama in Birmingham for assistance in computing.

References

Belford, G. G., Befford, R. L., & Weber, G. (1972) *Proc. Natl. Acad. Sci. U.S.A. 69*, 1392.

Berlman, I. B. (1971) in *Handbook of the Fluorescence Spectrum of Aromatic Molecules*, p 383, Academic Press, New York.

Björk, I., & Lindh, E. (1974) *Eur. J. Biochem. 45*, 135.

Brandtzaeg, P. (1975) *Scand. J. Immunol. 4*, 309.

Brochon, J. C., & Wahl, Ph. (1972) *Eur. J. Biochem. 25*, 20.

Chapuis, R. M., & Koshland, M. E. (1975) *Biochemistry 14*, 1320.

Cheung, H. C., & Morales, M. F. (1969) *Biochemistry 8*, 2177.

Chuang, T. J., & Eisenthal, K. B. (1972) *J. Chem. Phys. 57*, 5094.

Dale, R. E., & Eisinger, J. (1975) in *Biochemical Fluorescence: Concepts* (Chen, R., & Edelhoch, H., Eds.) Vol. 1, p 115, Marcel Dekker, New York.

Dudich, E. I., Nezlin, R. S., & Franek, F. (1978) *FEBS Lett. 89*, 89.

Ehrenberg, M., & Rigler, R. (1972) *Chem. Phys. Lett. 14*, 539.

Gafni, A., & Brand, L. (1976) *Biochemistry 15*, 3165.

Gottlieb, Y., & Wahl, Ph. (1963) *J. Chem. Phys. 60*, 849.

Grinvald, A. (1976) *Anal. Biochem. 75*, 260.

Habercom, M. S., & Cheung, H. C. (1978) *Arch. Biochem. Biophys. 191*, 756.

Harvey, S. C., & Cheung, H. C. (1977) *Biochemistry 16*, 5181.

Heremans, J. F. (1974) in *The Antigens II* (Sela, M., Ed.) p 365, Academic Press, New York.

Holowka, D. A., & Cathou, R. E. (1976) *Biochemistry 15*, 3379.

Kilian, M., Mestecky, J., & Schrohenloher, R. E. (1979) *Infect. Immun. 26*, 143.

Klotz, I. M. (1974) *Acc. Chem. Res. 7*, 162.

Knopp, J. A., & Weber, G. (1969) *J. Biol. Chem. 244*, 6309.

Liu, B. M., Cheung, H. C., Mestecky, J., & Harvey, S. C. (1977) *Biophys. J. 17*, 137a.

Lovejoy, C., Holowka, D. A., & Cathou, R. E. (1977) *Biochemistry 16*, 3668.

Marquardt, D. W. (1963) *J. Soc. Ind. Appl. Math. 11*, 431.

Melhuish, W. H. (1962) *J. Opt. Soc. Am. 52*, 1256.

Mestecky, J., Kulhavy, R., & Krause, F. W. (1972) *J. Immunol. 108*, 738.

Mestecky, J., Schrohenloher, R. E., Kulhavy, R., Weight, G. P., & Tomana, M. (1974) *Proc. Natl. Acad. Sci. U.S.A. 71*, 544.

Mestecky, J., Hammack, W. J., Kulhavy, R., Wright, G. P., & Tomana, M. (1977) *J. Lab. Clin. Med. 89*, 919.

Rigler, R., & Ehrenberg, M. (1976) *Q. Rev. Biophys. 10*, 1.

Rosenstein, R. W., & Jackson, P. (1973) *Biochemistry 12*, 1659.

Scatchard, G. (1949) *Ann. N.Y. Acad. Sci. 51*, 660.

Shinitzky, M. (1972) *J. Chem. Phys. 56*, 5979.

Tao, T. (1969) *Biopolymers 8*, 609.

Tumerman, I. A., Nezlin, R. S., & Zagyansky, Y. A. (1972) *FEBS Lett. 19*, 290.

Valentine, R. C., & Green, N. M. (1967) *J. Mol. Biol. 27*, 615.

Wahl, Ph., & Weber, G. (1967) *J. Mol. Biol. 30*, 371.

Wahl, Ph., Auchet, J. C., & Donzel, B. (1974) *Rev. Sci. Instrum. 45*, 23.

Weltman, J. K., & Edelman, G. M. (1967) *Biochemistry 6*, 1437.

Weltman, J. K., & Davis, R. P. (1970) *J. Mol. Biol. 54*, 177.

Yguerabide, J., Epstein, H. F., & Stryer, L. (1970) *J. Mol. Biol. 51*, 590.